

## Design of Propellant Composite Thermodynamic Properties Using Rocket Propulsion Analysis (RPA) Software

Anita Pinalia<sup>1)</sup>, Bayu Prianto<sup>1)</sup>, Henny Setyaningsih<sup>1)</sup>, Prawita Dhewi<sup>1)</sup>, and Ratnawati Ratnawati<sup>2, \*)</sup>

<sup>1)</sup> Center for Rocket Technology, National Research and Innovation Agency  
Jl. Raya Lapan No. 2, Mekarsari, Rumpin, Bogor 16350, Indonesia

<sup>2)</sup> Department of Chemical Engineering, Faculty of Engineering, Universitas Diponegoro  
Jl. Prof. Soedarto, SH, Tembalang, Semarang 50275, Indonesia

<sup>\*)</sup> Corresponding author: [ratnawati@che.undip.ac.id](mailto:ratnawati@che.undip.ac.id)

(Received: 27 June 2022; Published: 12 Juli 2022)

### Abstract

*Rocket Propulsion Analysis (RPA) is software for predicting the performance of a rocket engine. It is usually used in conceptual and preliminary design. Heat capacity and specific impulse are two properties related to the performance of a propellant. This work aimed to design AP/HTPB-based solid propellant composite with various compositions and predict the heat capacity and specific impulse using the RPA software. The materials used were ammonium perchlorate (AP) as the oxidizer, Hydroxy-Terminated Polybutadiene (HTPB) as the fuel binder, Al powder as the metal fuel, and other additives. Four propellants with different formulations were prepared and tested for heat capacity and specific impulse. The experimental heat capacity was obtained using a differential scanning calorimeter (DSC), while the specific impulse was obtained using a bomb calorimeter. The same propellant formulations were used as the input to the RPS to predict the heat capacity and specific impulse. The results show that the experimental heat capacity of the propellant ranges from 1.576 to 4.08 J g<sup>-1</sup> K<sup>-1</sup>, and the simulation result ranges from 1.78 to 3.48 J g<sup>-1</sup> K<sup>-1</sup>. The overall average deviation is 16.3%. The predicted specific impulse at vacuum and sea level ranges from 231.3 to 234.0 s and from 219.8 to 220.9 s, respectively. Meanwhile, the experimental specific impulse at vacuum and sea level varies from 236.2 to 240.3 s and from 228.5 to 232.9 s, respectively. The overall average deviation is 3.7%. Therefore, the RPA is reliable for predicting specific impulses of propellant, but it is not accurate enough for predicting the heat capacity of propellant composite.*

**Keywords:** composite propellant, heat capacity, specific impulse

**How to Cite This Article:** Pinalia, A., Prianto, B., Setyaningsih, H., Dhewi, P., & Ratnawati, R. (2022). Design of Propellant Composite Thermodynamic Properties Using Rocket Propulsion Analysis (RPA) Software. *Reaktor*, 22(1). <https://doi.org/10.14710/reaktor.22.1.1-6>

### INTRODUCTION

Composite propellants are solid propellants consisting of oxidizing agents, binders, fuels, and several additives. Ammonium perchlorate (AP) is widely used as the oxidizing agent, hydroxy-

terminated polybutadiene (HTPB) as the binder which is also consumed as fuel, and aluminum (Al) powder as the metal fuel. The addition of metal-fuel increases the flame temperature. The other additives used in the propellant manufacturing process are isophorone

diisocyanate (IPDI) as a curing agent and dioctyl adipate (DOA) as a plasticizer.

The efficiency of a rocket in terms of propulsion depends on the exhaust gas velocity and the mass ratio. Thrust is one of the important factors in the first stage of a rocket launching. All these parameters are determined by the rocket design and the propellant composition (Ghedjatti et al., 2020).

The composition of the propellant affects the physical, mechanical, and ballistic properties of the propellant. The physical and ballistic properties can be predicted using a thermodynamic characteristic approach. Rocket Propulsion Analysis (RPA) is software that can be used to predict the performance of a rocket engine. RPA is a user-friendly software, which provides a sufficient thermodynamics database. RPA is an analysis tool for the conceptual design of rocket propulsion systems. The RPA has been used to predict the specific impulse and heat capacity of propellants. The predicted specific impulse deviated only 0.2-1.3% compared to the experimental data. The heat capacities of three propellants predicted using the RPS were the same as those predicted using the NASA Computer program CEA2 (Chemical Equilibrium with Applications 2) (Ponomarenko, 2014).

The RPA can be used to design the propellant formulation with desired thermodynamics properties. The theoretical value of the thermodynamic property is calculated using RPA as a function of the key variables, such as the propellant composition, chamber pressure, and nozzle expansion ratio (Frank et al., 2015).

The examples of physical and ballistic properties of propellant are the heat capacity at constant pressure ( $C_p$ ) and the specific impulse ( $I_{sp}$ ), respectively. The heat capacity is an important property as it affects the rate of temperature rise at the startup transient of propellant combustion (Judd and Vernacchia, 2015). The specific impulse is a measure of the efficiency of rocket engines. It is directly linked to the thrust that a rocket motor develops (Frem, 2018). Both properties can be predicted using the RPA software.

To the best of our knowledge, there is only a limited number of publications about the prediction of the specific heat and the specific impulse of propellant using the RPA. Therefore, this work aimed to design propellants with various compositions, predict the  $C_p$  and  $I_{sp}$  of the propellants using the RPA software, and compare the predicted values to the experimental  $C_p$  and  $I_{sp}$ .

## MATERIALS AND METHOD

### Materials

The materials used in this work were ammonium perchlorate (AP), aluminum (Al) powder, hydroxyl-terminated polybutadiene (HTPB), dioctyl adipate (DOA), isophorone diisocyanate (IPDI), triphenyl bismuth (TPB), and maleic anhydride (MA). The AP, Al powder, HTPB, and DOA were purchased from Dalian Co. China. The IPDI was obtained from

the USA, while aziridine, TPB, and MA were from Hanwa, South Korea.

### Propellant preparation

The formulation of the propellants is presented in Table 1. The propellants were prepared by slurry casting technique (Aziz et al, 2012; O'Brien and Ryan, 2019). First, the binder HTPB and all other liquid ingredients were mixed and agitated using a glass rod. Al powder was then added and mixed well until all Al powder was coated by the binder. Then, AP was added and mixed well until a homogeneous slurry was obtained. The slurry was then cast in a vacuum casting device as depicted in Figure 1. The propellants were cured in an oven at 70°C for 3 × 24 hours. The propellants were ready for characterization.

Table 1. Propellant formulation

Component	Composition of propellants (% w)			
	P1	P2	P3	P4
AP	68.14	68.78	69.41	75.00
Al powder	15.00	15.00	15.00	7.41
HTPB	13.16	12.64	12.14	13.74
IPDI	1.32	1.28	1.23	1.37
TPB & MA	0.04	0.04	0.04	0.04
Aziridine	0.15	0.15	0.15	0.15
DOA	2.19	2.11	2.03	2.29



Figure 1. Vacuum casting device

### Propellant characterization

The propellants were tested for heat capacity ( $C_p$ ) and enthalpy of decomposition ( $\Delta H_{decomp}$ ). The heat capacity was determined using a differential scanning calorimeter (Shimadzu DSC-60). The DSC was operated at a constant heating rate (10°C min<sup>-1</sup>) and a maximum temperature of 550°C. The DSC generated heat transferred to the material to be tested at a rate of  $dQ/dt$ , causing an increase of the temperature at a heating rate of  $\beta$ . The heat capacity was calculated using Equation (1) (Cassel, 2001).

$$C_p = \frac{dQ/dt}{\beta w} \quad (1)$$

The heat of decomposition was determined using a bomb calorimeter (CAL3K-A DDS calorimeter). A sample of propellant was weighed and transferred to the vessel of the calorimeter. The vessel was then pressurized with nitrogen to 500 kPa before it was inserted into the bomb calorimeter, and the lid was closed to start the determination. The heat of

decomposition obtained was used to calculate the specific impulse ( $I_{sp}$ ) of the propellant at vacuum and sea level using Equations (2) and (3), respectively (Prianto et al., 2020)

$$I_{sp,vac} = \eta_{reaction} \eta_{nozzle} \sqrt{\frac{\Delta H_{decomp}}{g}} \quad (2)$$

$$I_{sp,sl} = I_{sp,vac} - P_{sl} \frac{A_e}{\dot{m}g} \quad (3)$$

**Propellant properties prediction**

The  $C_p$  and  $I_{sp}$  of the propellants were predicted using the RPA software. The formulation of the propellants (Table 1) was used as the input to the software.

**RESULTS AND DISCUSSION**

**Heat Capacity ( $C_p$ )**

The experimental heat capacity of the propellants at various temperatures is depicted in Figure 2 as a function of temperature. The data points for each propellant can be approximated well with straight lines represented by Equation (4) where a and b are constants. The values of a and b along with the coefficient of determination ( $R^2$ ) for the propellants are presented in Table 2. The coefficients of determination of all models are greater than 0.99, indicating that the equations fit well the experimental data.

$$C_p = a T + b \quad (4)$$

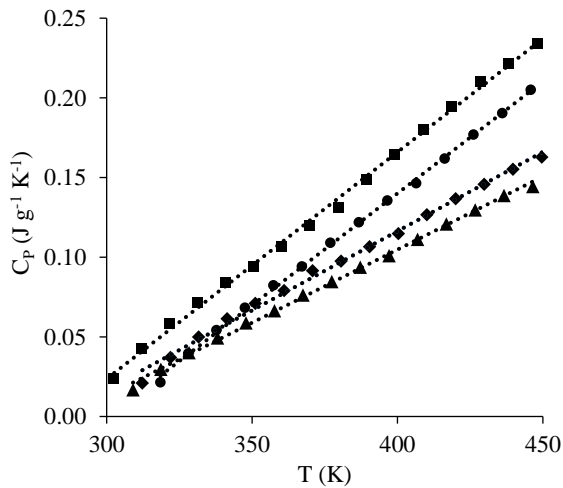


Figure 2. Linear Regression of Temperature (K) vs  $C_p$  ( $J g^{-1} K^{-1}$ ) for P1 (◆), P2 (▲), P3 (●), and P4 (■)

Table 2. Constants for the heat capacity equations

Propellant	a	b	$R^2$
P1	0.0010	-0.2815	0.9954
P2	0.0009	-0.2624	0.9982
P3	0.0014	-0.4213	0.9991
P4	0.0014	-0.4034	0.9980

The heat capacity of the propellant predicted using the RPA software varies with the composition of the propellant. The composition of the propellant affects the physical and mechanical properties as well

as combustion behavior of the propellant (Baht et al., 1986; Aziz et al., 2012; Chaturvedi and Dave, 2019). This is the reason why the temperatures at the nozzle inlet as well as at the nozzle exit are different for each propellant as shown in Figure 3. For example, the temperature at the nozzle inlet for propellant P1 is 3083.3 K, while that of propellant P2 is 3138.6 K.

Chamber Performance

Thermodynamic properties	Performance	Altitude performance	Throttled performance	
<b>Thermodynamic properties</b>				
Parameter	Injector	Nozzle inlet	Nozzle throat	Nozzle exit Unit
Pressure	7.0000	7.0000	3.9943	0.2434 MPa
Temperature	3083.0907	3083.0907	2862.2008	1973.3017 K
Enthalpy	-2035.9579	-2035.9579	-2569.7349	-4700.9085 kJ/kg
Entropy	9.7259	9.7259	9.7259	9.7259 kJ/(kg-K)
Internal energy	126.0576	126.0576	-160.7935	-1245.0141 kJ/kg
Specific heat (p=const)	2.8015	2.8015	2.5071	1.8540 kJ/(kg-K)
Specific heat (V=const)	2.4031	2.4031	2.1384	1.5337 kJ/(kg-K)
Gamma	1.1658	1.1658	1.1724	1.2088
Isentropic exponent	1.1583	1.1583	1.1678	1.2086
Gas constant	0.3208	0.3208	0.3194	0.3173 kJ/(kg-K)
Molecular weight (M)	25.9205	25.9205	26.0312	26.2043

(a)

Chamber Performance

Thermodynamic properties	Performance	Altitude performance	Throttled performance	
<b>Thermodynamic properties</b>				
Parameter	Injector	Nozzle inlet	Nozzle throat	Nozzle exit Unit
Pressure	7.0000	7.0000	4.0005	0.2468 MPa
Temperature	3138.6004	3138.6004	2920.3506	2041.6350 K
Enthalpy	-2040.8463	-2040.8463	-2575.2376	-4711.0059 kJ/kg
Entropy	9.6937	9.6937	9.6937	9.6937 kJ/(kg-K)
Internal energy	88.2497	88.2497	-201.6566	-1293.1082 kJ/kg
Specific heat (p=const)	2.8774	2.8774	2.5782	1.8746 kJ/(kg-K)
Specific heat (V=const)	2.4731	2.4731	2.2056	1.5580 kJ/(kg-K)
Gamma	1.1625	1.1625	1.1690	1.2032
Isentropic exponent	1.1549	1.1549	1.1634	1.2029
Gas constant	0.3161	0.3161	0.3146	0.3121 kJ/(kg-K)
Molecular weight (M)	26.3066	26.3066	26.4304	26.6424

(b)

Chamber Performance

Thermodynamic properties	Performance	Altitude performance	Throttled performance	
<b>Thermodynamic properties</b>				
Parameter	Injector	Nozzle inlet	Nozzle throat	Nozzle exit Unit
Pressure	7.0000	7.0000	4.0066	0.2501 MPa
Temperature	3191.8078	3191.8078	2976.5074	2110.0528 K
Enthalpy	-2045.6688	-2045.6688	-2580.2102	-4718.3331 kJ/kg
Entropy	9.6598	9.6598	9.6598	9.6598 kJ/(kg-K)
Internal energy	51.2521	51.2521	-241.1587	-1338.4773 kJ/kg
Specific heat (p=const)	2.9617	2.9617	2.6579	1.9020 kJ/(kg-K)
Specific heat (V=const)	2.5501	2.5501	2.2901	1.5881 kJ/(kg-K)
Gamma	1.1614	1.1614	1.1657	1.1975
Isentropic exponent	1.1515	1.1515	1.1591	1.1969
Gas constant	0.3115	0.3115	0.3099	0.3069 kJ/(kg-K)
Molecular weight (M)	26.6949	26.6949	26.8321	27.0878

(c)

Chamber Performance

Thermodynamic properties	Performance	Altitude performance	Throttled performance	
<b>Thermodynamic properties</b>				
Parameter	Injector	Nozzle inlet	Nozzle throat	Nozzle exit Unit
Pressure	7.0000	7.0000	3.9454	0.1013 MPa
Temperature	2775.3582	2775.3582	2528.4232	1337.1031 K
Enthalpy	-2244.3236	-2244.3236	-2761.1414	-5127.5608 kJ/kg
Entropy	10.0381	10.0381	10.0381	10.0381 kJ/(kg-K)
Internal energy	-1616.3330	-1616.3330	-1979.8459	-3564.4010 kJ/kg
Specific heat (p=const)	2.2366	2.2366	2.0796	1.7841 kJ/(kg-K)
Specific heat (V=const)	1.8699	1.8699	1.7263	1.4449 kJ/(kg-K)
Gamma	1.1961	1.1961	1.2046	1.2348
Isentropic exponent	1.1935	1.1935	1.2034	1.2348
Gas constant	0.3403	0.3403	0.3397	0.3392 kJ/(kg-K)
Molecular weight (M)	24.4306	24.4306	24.4744	24.5152

(d)

Figure 3. RPA Simulation results for predicting specific heat of propellant P1 (a), P2 (b), P3 (c), and P4 (d)

The heat capacity predicted by the RPA software was compared to those of the experimental values. As shown in Figure3, the heat capacities of the propellants at the nozzle inlet and exit are at very high temperatures (1337.1 – 3191.8 K), while the experimental heat capacities are at much lower temperatures (300 – 450 K). Therefore, the experimental heat capacities of each propellant were extrapolated using Equation (4). The results are presented in Figures 4 and 5 for the heat capacity of propellants at the inlet and exit of the nozzle, respectively.

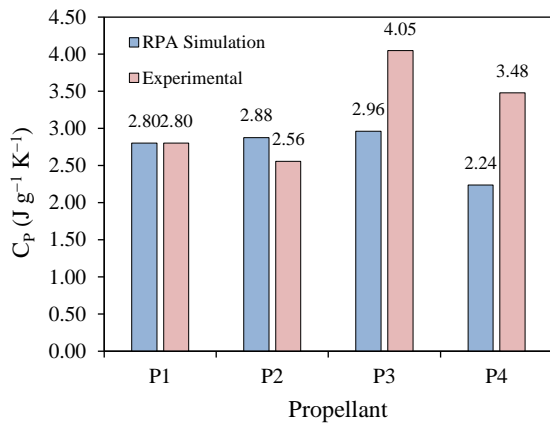


Figure 4. Simulated and experimental heat capacity of propellant at the nozzle inlet

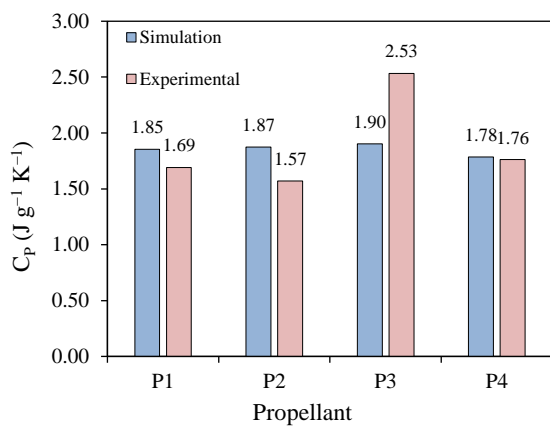


Figure 5. Simulated and experimental heat capacity of propellant at the nozzle exit

Figure 4 shows that the experimental value of  $C_p$  of the propellant at the nozzle inlet (at 2775.4 – 3191.8 K) ranges from 2.56 – 4.08 J g<sup>-1</sup> K<sup>-1</sup>, while those of the simulation result range from 2.24 – 3.48 J g<sup>-1</sup> K<sup>-1</sup>. The  $C_p$  of P1 and P2 at the nozzle inlet of RPA simulation is close to the experimental results, while the simulation results for propellants P3 and P4 are lower than those of the experimental values.

The temperature at the nozzle exit varies from 1337.1 to 2110.0 K. The variation of temperature and composition of the propellants caused the variation of  $C_p$  from 1.78 to 1.90 J g<sup>-1</sup> K<sup>-1</sup> for the simulation results and from 1.57 to 2.53 J g<sup>-1</sup> K<sup>-1</sup> for the experimental results, as shown in Figure 5. The simulated values of  $C_p$  of propellant P1, P2, and P4 are close enough to the experimental results, while that of propellant P3 is lower than the experimental  $C_p$ .

The overall average absolute deviation of the simulated heat capacity compared to the experimental values is 16.3%. It can be caused by several factors one of which is the inhomogeneity in the blending of the propellant ingredient during propellant preparation which may lead to the formation of voids inside the propellant composite. The inhomogeneity and the existence of voids may affect the heat transfer inside

the propellant and the combustion performance of the propellant (Kohga, 2007).

Ponomarenko (2014) predicted the heat capacities of three propellants using the RPA. They reported that the heat capacity of propellant 1 at 3523.8 K, propellant 2 at 3723.6 K, and propellant 3 at 3392.3 K were 8.2367, 6.0260, and 5.296 J g<sup>-1</sup> K<sup>-1</sup>, respectively. However, there was no information about the compositions of the propellants.

Estimated delivered performance				
Reaction efficiency:	0.9200			
Nozzle efficiency:	0.9558			
Overall efficiency:	0.8793			
Parameter	Sea level	Optimum expansion	Vacuum	Unit
Characteristic velocity		1426.56		m/s
Effective exhaust velocity	2155.71	1997.39	2268.60	m/s
Specific impulse (by mass)	2155.71	1997.39	2268.60	N-s/kg
Specific impulse (by weight)	219.82	203.68	231.33	s
Thrust coefficient	1.5111	1.4001	1.5903	

(a)

Estimated delivered performance				
Reaction efficiency:	0.9200			
Nozzle efficiency:	0.9559			
Overall efficiency:	0.8795			
Parameter	Sea level	Optimum expansion	Vacuum	Unit
Characteristic velocity		1430.51		m/s
Effective exhaust velocity	2161.65	1999.14	2274.85	m/s
Specific impulse (by mass)	2161.65	1999.14	2274.85	N-s/kg
Specific impulse (by weight)	220.43	203.86	231.97	s
Thrust coefficient	1.5111	1.3975	1.5902	

(b)

Estimated delivered performance				
Reaction efficiency:	0.9200			
Nozzle efficiency:	0.9561			
Overall efficiency:	0.8796			
Parameter	Sea level	Optimum expansion	Vacuum	Unit
Characteristic velocity		1433.79		m/s
Effective exhaust velocity	2166.60	1999.94	2280.06	m/s
Specific impulse (by mass)	2166.60	1999.94	2280.06	N-s/kg
Specific impulse (by weight)	220.93	203.94	232.50	s
Thrust coefficient	1.5111	1.3949	1.5902	

(c)

Estimated delivered performance				
Reaction efficiency:	0.9200			
Nozzle efficiency:	0.9629			
Overall efficiency:	0.8859			
Parameter	Sea level	Optimum expansion	Vacuum	Unit
Characteristic velocity		1379.08		m/s
Effective exhaust velocity	2105.81	2105.81	2294.66	m/s
Specific impulse (by mass)	2105.81	2105.81	2294.66	N-s/kg
Specific impulse (by weight)	214.73	214.73	233.99	s
Thrust coefficient	1.5270	1.5270	1.6639	

(d)

Figure 6. RPA Simulation results for predicting specific impulse of propellant P1 (a), P2 (b), P3 (c), and P4 (d)

### Specific Impulse ( $I_{sp}$ )

The specific impulse of a rocket motor is one of the most important factors determining its overall performance. It is usually used as an indicator of the efficiency of a propellant. The specific impulse measures the amount of thrust generated over a given time per weight of propellant consumed (Frem, 2018; O'Brien and Ryan, 2019). The output of the RPA software for predicting the specific impulse of the propellants is depicted in Figure 5.

The experimental value of heat of decomposition was determined using the bomb calorimeter. Table 3 lists the experimental heat of decomposition of the propellants. The experimental heat of decomposition along with the reaction and nozzle efficiency from Figure 6 was used to calculate the specific impulse according to Equations (2) and (3). The results (denoted as the experimental  $I_{sp}$ ) along with the simulation results are presented in Figures 8 and 9 for the  $I_{sp}$  at vacuum and sea level, respectively.

Table 3. Experimental heat of decomposition

Propellant	$\Delta H_{decomp}$ (MJ kg <sup>-1</sup> )
P1	6.98
P2	6.91
P3	7.10
P4	7.05

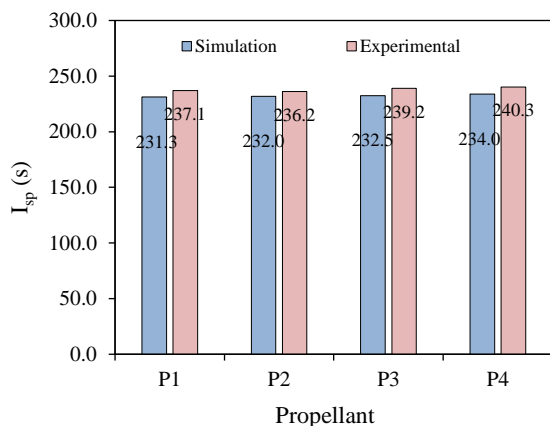


Figure 7. The simulated and experimental specific impulse of propellant at vacuum

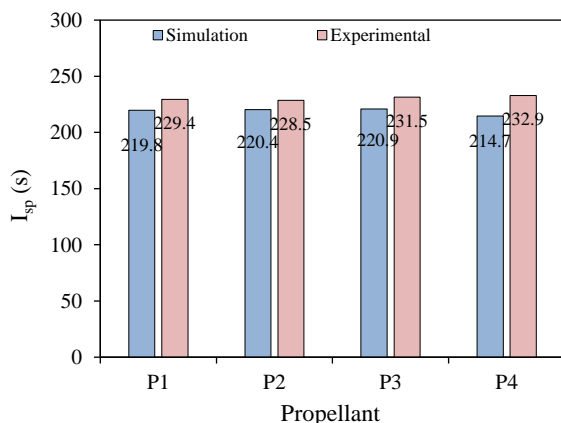


Figure 8. The simulated and experimental specific impulse of propellant at sea level

As seen in Figure 7, the simulation result of the specific impulse of the propellant at vacuum ranges from 231.3 to 234.0 s. The experimental values of specific impulse are slightly higher than the predicted values, i.e., they range from 236.2 to 240.3 s. The specific impulse at sea level has the same trend as the specific impulse at vacuum. The simulation result of specific impulse ranges from 219.8 to 220.9 s, while those of the experimental values range from 228.5 to 232.9 s. The differences between the simulation and experiment values could be caused by several factors relating to propellant preparation. Inhomogeneity that might occur during the blending of all propellant ingredients could lead to void formation. It can affect the performance of the propellant (Kohga, 2007), one of which is indicated by its specific impulse. However, the overall average deviation is only 3.7%. Hence, the RPA software is reliable enough for predicting the specific impulse of solid propellant.

Ponomarenko (2014) predicted the specific impulses of three rocket engines using the RPA. They found that the specific impulses at vacuum ranged from 314.7 to 449.2 s, while those at sea level ranged from 282.2 to 367.9 s. Compared to the actual specific impulses of the rocket engines, the predicted values deviated only 0.58% on average.

O'Brien and Ryan (2019) measured the specific impulse of AP/HTBP-based solid propellant with three formulations. They found that the specific impulses of the propellants were 176 – 195 s. They used ProPEP software to predict the specific impulse and they found the values as 182 – 219 s with an overall average deviation of 6.1%.

### CONCLUSION

Prediction of the heat capacity and the specific impulse of AP-based solid propellant has been conducted using the RPA software. An experimental determination of the heat capacity and the specific impulse of the propellant was performed as well. The results show that the experimental heat capacity of the propellant at the nozzle inlet ranges from 2.56 to 4.08 J g<sup>-1</sup> K<sup>-1</sup>, and the simulation result ranges from 2.24 to 3.48 J g<sup>-1</sup> K<sup>-1</sup>. In the nozzle exit, the experimental and simulated heat capacity range from 1.57 to 2.53 J g<sup>-1</sup> K<sup>-1</sup> and from 1.78 to 1.90 J g<sup>-1</sup> K<sup>-1</sup>, respectively. The overall average deviation is 16.3%. The specific impulse at vacuum predicted using the RPA software ranges from 231.3 to 234.0 s, while the experimental results range from 236.2 to 240.3 s. The specific impulse at sea level predicted using the RPA software ranges from 219.8 to 220.9 s, while the experimental results range from 228.5 to 232.9 s. The predicted specific impulses, both at vacuum and sea level, are lower than the experimental results. The overall average deviation is 3.7%. The RPA software is reliable for predicting the specific impulse.

**NOTATION**

$A_e$	: cross-sectional area of the nozzle exit [ $m^2$ ]
$C_p$	: constant-pressure heat capacity [ $J g^{-1} K^{-1}$ ]
$dQ/dt$	: heat flow [ $J s^{-1}$ ]
$g$	: gravitational acceleration [ $m s^{-2}$ ]
$I_{sp,sl}$	: specific impulse at sea level [s]
$I_{sp,vac}$	: specific impulse at vacuum [s]
$P_{sl}$	: pressure at sea level [Pa]
$T$	: temperature [K]
$w$	: weight of sample [g]
$\Delta H_{decomp}$	: heat of decomposition [ $J g^{-1}$ ]
Greek letters	
$\beta$	: heating rate [ $K s^{-1}$ ]
$\eta$	: efficiency

**ACKNOWLEDGEMENT**

This work was funded by the National Institute of Aeronautics and Space (LAPAN-Indonesia). The authors would like to thank Lilis Mariani, Head of Rocket Technology Centre – LAPAN for supporting this research.

**REFERENCES**

- Aziz, A., Mamat, R., Amin, M., and Wan Ali, W. K., (2012), Effect of Propellant Composition to the Temperature Sensitivity of Composite propellant, *IOP Conf. Series: Materials Science and Engineering*, 36, 012023.
- Baht, V. K., Singh, H., Khare, R. R., and Rao, K. R. K., (1986), Burning Rate Studies of Energetic Double Base Propellant, *Defence Science Journal*, 36(1), 71-75.
- Cassel, R. B. (2001). How Tzero™ Technology Improves DSC Performance Part III: The Measurement of Specific Heat Capacity. TA279, 1–4. <http://www.tainstruments.com/pdf/literature/TA279.pdf> (downloaded on February 10, 2022).
- Chaturvedi, S., and Dave, N. P., (2019), Solid Propellants: AP/HTPB Composite Propellants, *Arabian Journal of Chemistry*, 12, 2061-2068.
- Frank, C. P., Tyl, C. M., Pinon-Fischer, O. J., and Mavris, D. N., (2015), New Design Framework for Performance, Weight and Life-Cycle Cost Estimation of Rocket Engines, *6<sup>th</sup> European Conference for Aerospace Sciences*.
- Frem, D., (2018), A Reliable Method for Predicting the Specific Impulse of Chemical Propellants, *Journal of Aerospace Technology and Management*, 10, 1–21.
- Ghedjatti, I., Yuan, S., & Wang, H., (2020). Thermodynamic Investigation of Conventional and Alternative Rocket Fuels for Aerospace Propulsion. *IOP Conference Series: Materials Science and Engineering*, 887(1).
- Judd, S. and Vernacchia, M., (2015), 2.28 Final Report Solid Rocket Propellant Combustion, [https://mvernacc.github.io/portfolio/assets/docs/2.28/228\\_final\\_report.pdf](https://mvernacc.github.io/portfolio/assets/docs/2.28/228_final_report.pdf) (downloaded on February 4, 2022).
- Kohga, M., (2007), Effect of Voids inside AP Particles on Burning Rate of AP/HTPB Composite Propellant, *Propellants, Explosives, Pyrotechnics*, 33(4), 249-254.
- O'Brien, I., and Ryan, A., (2019), Improving the Delivered Specific Impulse of Composite Rocket Propellant through Alteration of Chemical Composition: Methodology and Parameters for Characterization of Propellant and Validation of Simulation Software Common to the Amateur Rocketry Community, *The University of Akron*, [https://ideaexchange.uakron.edu/cgi/viewcontent.cgi?article=1843&context=honors\\_research\\_projects](https://ideaexchange.uakron.edu/cgi/viewcontent.cgi?article=1843&context=honors_research_projects) (downloaded on February 5, 2022).
- Ponomarenko, A., (2014), RPA-Tool for Rocket Propulsion Analysis. *Space Propulsion Conference*.
- Prianto, B., Setyaningsih, H., and Puspitasari, R. R., (2020), Analysis of Composite Propellant Energy and Correlation with Specific Impulse at Vacuum Level. *Proceeding of The 7th International Seminar on Aerospace Science and Technology (ISAST 2019)*, 2232(April), 040011.